

The LINC-NIRVANA fringe and flexure tracker: control design overview

Steffen Rost^a and Andreas Eckart^a and Matthew Horrobin^a and Bettina Lindhorst^a and Uwe Lindhorst^a and Lydia Moser^a and Semir Smajic^a and Christian Straubmeier^a and Evangelia Tremou^a and Imke Wank^a and Jens Zuther^a and Thomas Bertram^b

^aI. Physics Institute, University of Cologne, Zùlpicher Str. 77, 50937 Cologne, Germany;

^bMax Planck Institute for Astronomy, Königstuhl 17, 69117 Heidelberg, Germany

ABSTRACT

The Fringe and Flexure Tracker System (FFTS) of the LINC-NIRVANA instrument is designed to monitor and correct the atmospheric piston variations and the instrumental vibrations and flexure at the LBT during the NIR interferometric image acquisition. In this contribution, we give an overview of the current FFTS control design, the various subsystems, and their interaction details. The control algorithms are implemented on a real-time computer system with interfaces to the fringe and flexure detector read-out electronics, the OPD vibration monitoring system (OVMS) based on accelerometric sensors at the telescope structure, the piezo-electric actuator for piston compensation, and the AO systems for offloading purposes. The FFTS computer combines data from different sensors with varying sampling rate, noise and delay. This done on the basis of the vibration data and the expected power spectrum of atmospheric conditions. Flexure effects are then separated from OPD signals and the optimal correcting variables are computed and distributed to the actuators. The goal is a 120 nm precision of the correction at a bandwidth of about 50 Hz. An end-to-end simulation including models of atmospheric effects, actuator dynamics, sensor effects, and on-site vibration measurements is used to optimize controllers and filters and to pre-estimate the performance under different observation conditions.

Keywords: LBT, LINC-NIRVANA, fringe tracking, piston, control

1. INTRODUCTION

The Fringe and Flexure Tracking System^{1,2} (FFTS) is an integral part of LINC-NIRVANA^{3,4}. It monitors the beams of the two arms of the Large Binocular Telescope (LBT) and takes action that they are combined in the same spot of the science detector. Furthermore its purpose is to detect the optical path difference (OPD) between incoming wavefronts of the the two interferometric channels. A moving mirror is used to introduce differential piston and compensate these effects. Driven in a closed-loop^{5,6} by monitoring the PSF of a reference star, the FFTS provides interferometric observations with a maximum fringe contrast. However, to achieve a large sky-coverage and to allow universal observing conditions, the tracking star can be chosen to be far away from the science target (up to 30") and the filter for observing the tracking star can be different from the science filter.^{2,7} This, the dispersion effects from the atmosphere and technical obstacles like inevitable delays, limited frame rates, sensitivity and precision of actuators, have great impact on the resulting performance, i. e. the fringe contrast. With a sophisticated control design we try to separate different task of the system to keep things as simple as possible, and thus stable, without losing performance and still allow multiple observing conditions.

2. CONTROL OVERVIEW

The fringe and flexure control loops are implemented on a real-time Linux system, a multiprocessor computer powerful enough for the image processing and piston calculations. The real-time extensions of current Linux kernels have proven to be sufficient for these control tasks.⁸ The system and the interfaces to the various subsystems including sensors and actuators are shown in figure 1.

Further author information: (Send correspondence to S. Rost: E-mail: rost@ph1.uni-koeln.de, Telephone: +49 (0)221 470-3548

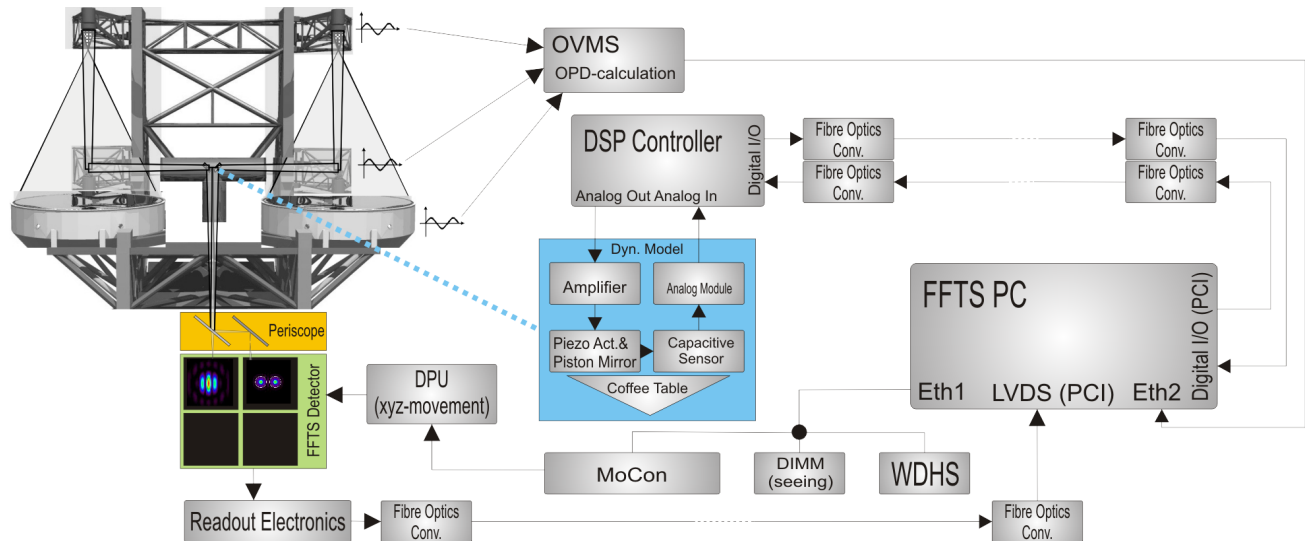


Figure 1. Overview of fringe control design: The actuator for the compensation of optical path difference (OPD) is the piston mirror. For the optimization of the dynamical behavior of the actuator it is important to model also the interfaces, sensors and mounting of the system.

2.1 Flexure Control

The position on the detector of the two spots of the tracking star have to be adjusted very precisely for the interferometric combination of light. Assuming the AO produces good corrections for the two telescopes, deformations of the resulting PSF can occur because: there is OPD in combination with atmospheric dispersion effects,⁹ or the centers of the two beams are deviating. To exactly determine flexure effects a dedicated slow motion channel, i. e. a separate detector quadrant is used, providing separate spots of the tracking star through a periscope. This optical device splits the incoming light beams into the fringe and the flexure channel with a fraction of 1:9. Details of the opto-mechanical concept are given in Zuther et al.⁹ In the flexure channel the central position of the separated spots can be monitored and differential flexure or common mode flexure can be detected. This is supposed to happen on a large timescale (of about seconds), as the telescope structure is moved, e. g. when the elevation is changed. For compensation of differential and common mode flexure actuators of the AO system, such as the deformable secondary mirrors are addressed (cf. Fig. 3).

2.2 Fringe Control

The OPD is changing on a smaller timescale, due to atmospheric effects and vibrations of the telescope and instrument. Therefore a higher read-out frequency in the fringe channel is needed, implying a decreased SNR, or in other words a decreased maximum magnitude for the tracking star. The design of the LINC-NIRVANA instrument allows different bandpass filters for the fringe and flexure detector and the science detector by reflecting the light with a dichroic mirror.¹⁰ The piston increases from lower wavelength to higher wavelength, which has to be considered in the error budget. Also the separation between science target and tracking star has an impact on the corresponding PSFs with the differential piston angular anisoplanatism,² which is related to the atmospheric conditions and the performance of the AO.

Another effect on the resulting PSF and the fringe contrast is the atmospheric differential refraction, depending on the zenith distance of the target. Dispersion distortions of the PSF can be used to detect OPD and find the zeroth fringe. There again the SNR is reduced since the light is spread on the detector by dispersion (cf. Fig. 4). Hence the current filter wheel and periscope design allows to compensate or introduce dispersion by wedges.⁹

Depending on the observing conditions, the performance of the AO corrections will vary. The image characteristics are very important for the applicable PSF fitting algorithm to precisely determine the actual OPD. Horrobin et al.¹¹ conducted a detailed study of the expected PSF by simulating atmospheric effects with the

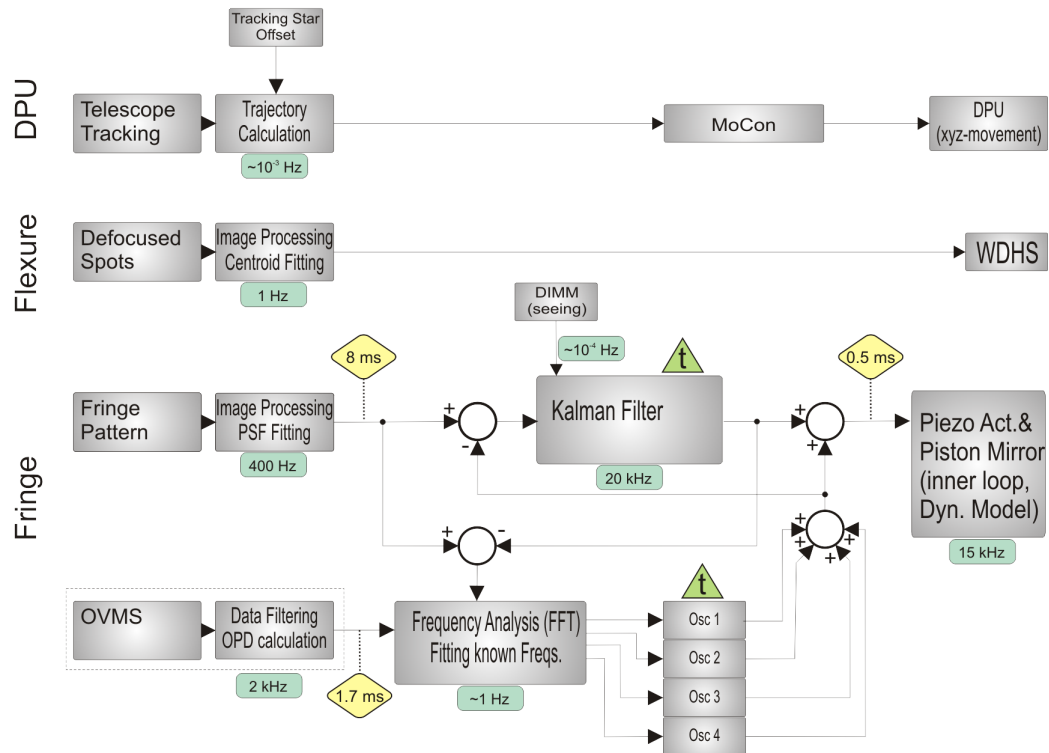


Figure 2. Control loops of the FFTS. The detector positioning unit (DPU, driven by a standalone motor controller MoCon) control and the flexure control loop are mostly separated from other subsystems. The fringe control is more complex, as the OVMS and the PSF fitting both detect OPD from different sources and are combined in nested loops. Noted are some critical latencies for sensor data, and the loop frequencies. In the Kalman filter and the vibration oscillators these delays are compensated by predicting OPD states (marked with a t in a triangle).

LOST package¹² and outline the requirements for a robust and sensitive algorithm, which can be used under different observing conditions.

2.3 Piston Mirror

The piston mirror is the most critical actuator for the OPD control. The dynamical behavior and the precision at getting to the set-point, which is calculated by the fringe control loop, directly affects the performance. As a goal the residual OPD on the science detector should not exceed 0.1λ or about 120nm. This performance allows high quality observations with sophisticated image reconstruction techniques.¹³ Therefore much effort has been devoted to the optimization of the so-called inner control loop. The inner loop consists of (cf. Fig. 1):

- piston mirror
- piezo-electric actuator stage with capacitive position sensor
- voltage amplifier driving the piezo
- analog module reading the position signal
- coffee table, i. e. the mounting structure
- DSP controller

It is important to consider the whole system at the optimization process to include the dynamical characteristics of each subsystem. For example the coffee table has shown a typical resonance frequency in measurements,

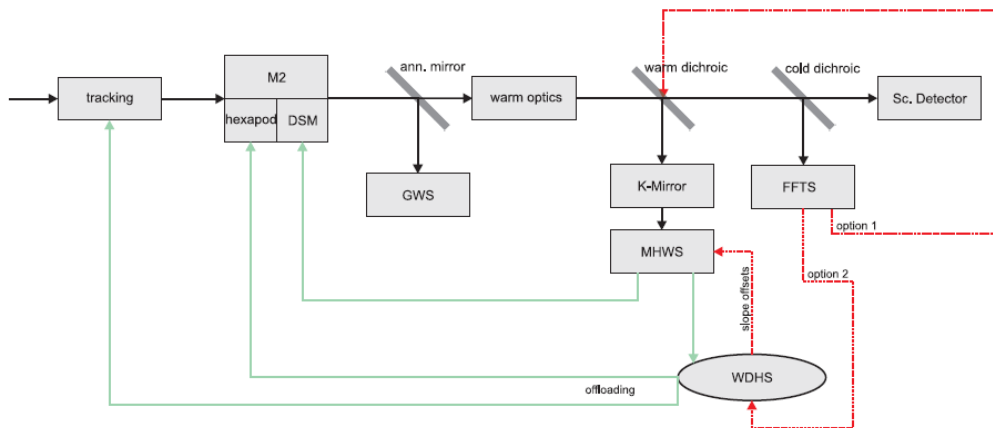


Figure 3. Control scheme for slow image motion tracking. Flexure effects at a rate of ~ 1 Hz are detected by the flexure channel of the FFTS. For the correction of misaligned beams the wavefront data handling system (WDHS) as part of the AO is addressed. Actuators of the deformable secondary mirrors or on the (warm) optical bench of LINC-NIRVANA

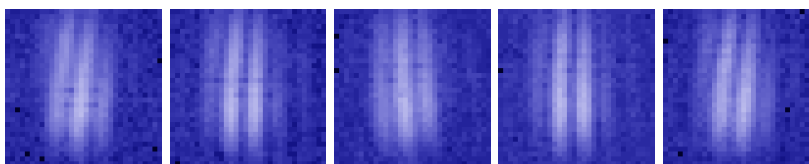


Figure 4. PSF images from FFTS detector: Visible are atmospheric dispersion effects, as the fringes are inclined. The images are taken in a laboratory experiment with the FFTS detector, so the noise shows a realistic behavior and the moving reset line is observable.

although it is optimized in terms of stiffness and is equipped with additional support structures. The piezo actuators resonance frequency is dependant on the load, and the piston mirror can not be made smaller due to the optical design of LINC-NIRVANA.⁴ With the optimal design control method \mathcal{H}_∞ the performance could be improved in comparison to a classic PID control approach.⁶ Details of the inner loop measurements and control design can be found in Brix et al.¹⁴

2.4 FFTS detector

Simulations of the AO performance under realistic atmospheric conditions propose a merely uncritical atmospheric OPD variation in terms of dynamics.^{6,11} The complexity for the control loop arises from the additional instrumental OPD and varying OPD fit quality. Horrobin et al.¹¹ found, that all simple PSF fitting algorithms relying on the position of the 8m-PSF with respect to the fringe pattern will not work under typical AO performance. Therefore a high sampling rate of the OPD signal of several hundred Hertz is needed.⁶ As the fringe channel and the flexure channel are both located on the same detector with a single read-out electronics board (cf. Fig. 1), a special read-out pattern was developed to provide both a high read-out frequency for the fringe channel, good SNR and long integration time on the flexure channel. A specific feature of this read-out mode is a moving line reset, which allows higher sampling rates, but slightly distorts the images (cf. Fig. 4). Not every frame will deliver the same quality measurement of OPD, as noise, reset line, and AO effects will vary. The goal for the control bandwidth is 50 Hz, as all atmospheric and so far known vibrational OPD could be handled (cf. Fig. 5). This implies a sampling frequency of at least 100 Hz and because of the mentioned obstacles (image quality, noise, latency) oversampling is necessary. The fringe control loop is designed to handle images at rates up to 400 Hz, depending on the magnitude of the tracking star and the SNR.

The detector will be positioned in the focal plane with a field of view of up to $60'' \times 90''$, limited by the isopiston patch.¹ This is achieved with the detector positioning unit (DPU), a 3D-stage with high positional repeatability. The position control of the DPU during an observation is fundamental for the fringe control, as the fringe pattern of the tracking star must be visible in a small window of 32×32 pixel in all frames. An even

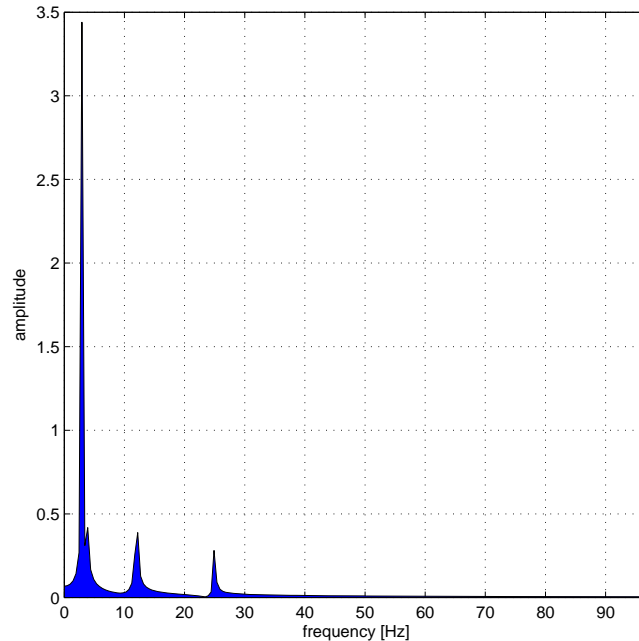


Figure 5. FFT power spectrum of LBT vibrations: The OVMS data is buffered for about 10 seconds, so that the FFT spectral analysis provides very precise estimates of the critical frequencies. In this example taken from preliminary measurements four frequencies can be identified. These are then fed into the vibration fitting, which in turn delivers delay-compensated sinusoids of correct phase and amplitude to predict the current vibrational OPD states.

more accurate position may have positive effects on the PSF fitting,⁷ so that the goal for the positioning in the focal plane is sub-pixel precision, i. e. about $4 \mu\text{m}$. After the trajectory for an observation is calculated, the DPU position control loop is mostly independent of the other loops (cf. Fig. 2), if the precision is maintained, e. g. also if the inclination is changing. Tremou et al.¹⁵ conducted DPU positioning tests with high precision measurement equipment.

2.5 OVMS

A considerable effort has been made in the past to monitor, characterize, and understand the vibrational behavior of the LBT, which is crucial for the performance of many instruments at the LBT, especially the interferometers like LINC-NIRVANA.^{10,16} Vibrations were measured with different methods, e. g. with optical vibrometers or piezoelectric accelerometers, on different spots of the structure, and in different operating modes of the telescope, i. e. with subsets of actuator and facility devices operating during an observation.¹⁷ This gives the opportunity to compensate vibrations, e. g. passively by adding support structures. This is an ongoing process, as more and more sources of vibrations are identified. A number of accelerometers with corresponding cabling were installed permanently to the telescope structure, where the movement is critical to the OPD, like the swing arms with secondary or tertiary mirrors. The OPD vibration monitoring system (OVMS) collects all these sensor data and distributes them to various subsystems of the instruments. It consists of a DSP with analog inputs, which is applying basic filters to the measured data. To achieve a low latency, the data is sent over a dedicated Ethernet port to the FFTS computer. First tests show a latency of about 1.8 ms. From the filtered accelerometer data critical OPD frequencies can be derived directly. For further information including amplitudes and phases, the time signal has to be integrated twice. Details of these calculations and applicable filtering techniques can be found in Brix et al.¹⁴

For the performance of the fringe tracking it is important to know about the critical frequencies in advance. Figure 7 shows, that a good fit can be achieved with known frequencies as fixed parameters. This vibration state, i. e. the phases, amplitudes, and frequencies, is considered to be constant at least on a time scale of several seconds, as preliminary measurements in different operational modes of the telescope indicate. A time series of

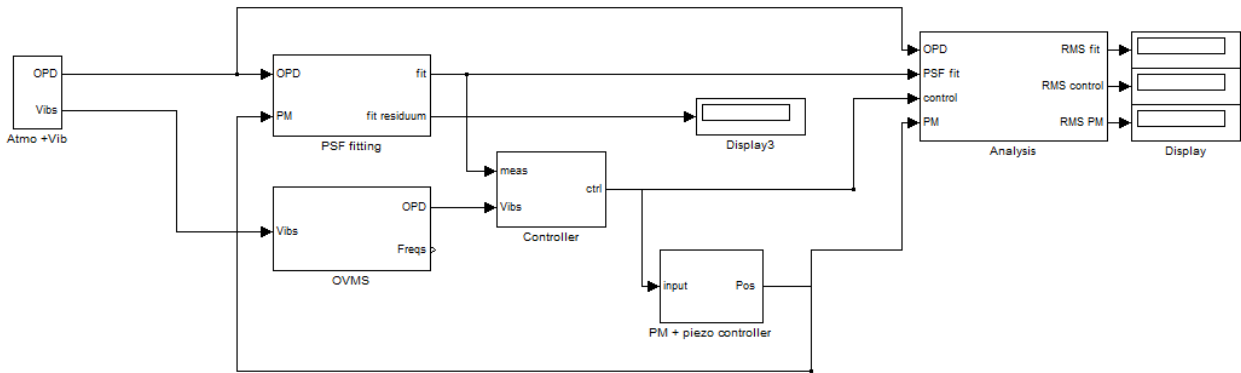


Figure 6. Matlab/Simulink model. In the simulation all critical aspects of the control loops are modeled, e. g. latencies of the image acquisition and PSF fitting, noise effects of sensors and the actuator dynamics.

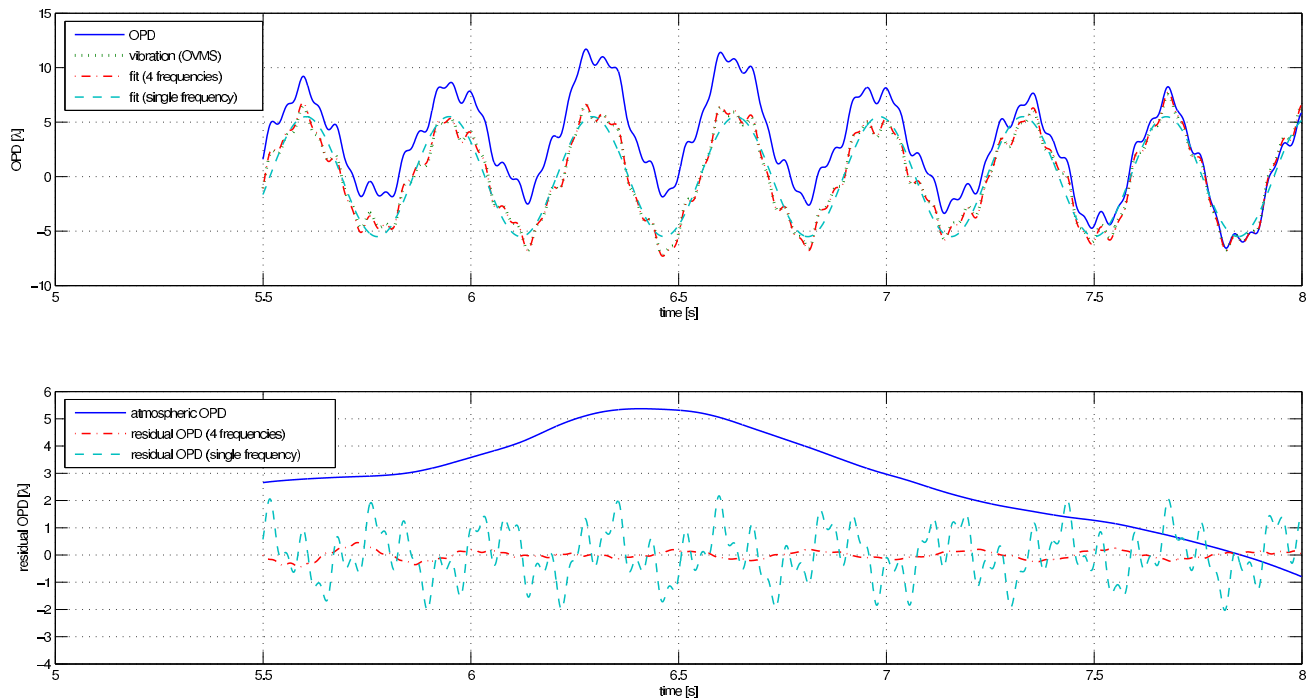


Figure 7. Vibration Control with OVMS data: the OVMS data is fitted with a single or multiple sinusoids. At the top the total OPD is shown and with a dotted line the OVMS data. To the bottom the residual OPD is shown, the solid line is the pure atmospheric OPD, without the vibrational OPD, the dashed lines are the residuals of the fits. Note that these errors are partially corrected in the other fringe control loop by the Kalman filter (cf. Fig. 2).

buffered OVMS data of 10 seconds can be used to verify the vibration state by spectral analysis (FFT, cf. Fig. 5).

3. SIMULATION

We are currently setting up a simulation tool, which covers all important aspects of the FFTS. The input images are simulated with the LOST package.¹² The code is extended and modified to include important effects of the AO correction for the fringe fitting, including atmospheric dispersion. The images are pre-computed for a time series of atmospheric OPD for typical observing conditions⁶ and for different zenith angles, i. e. atmospheric dispersion. For instrumental OPD a vibration state is chosen, based on the on-site measurements of the telescope structure. The PSF images and the vibration state are read by a Matlab/Simulink block set, which is shown

in figure 6. This tool allows to estimate the achievable residual piston under varying observing conditions. The following issues are modeled explicitly in the simulation:

- latency of the detector read-out of PSF images
- noise of PSF images (realistic detector noise, including moving reset line, dead pixels, etc.)
- sampling rate of PSF images
- read-out pattern effects
- latency of fringe fitting
- latency of OVMS data
- noise of OVMS data from accelerometers and OPD calculation error
- sampling rate of OVMS data
- dynamical model of piston mirror, piezo actuator, DSP controller, coffee table
- latency of the interface to the piston mirror controller

The interface to the piston mirror controller is a digital I/O card on the FFTS PC with fiber optics transmission boxes as shown in figure 1. The quite long distance to the DSP controller is bridged with a high bandwidth and very low latency of about 300 ns. The control loops are designed as shown in figure 2. The atmospheric OPD is calculated by subtracting the current vibration state and then fed into a Kalman filter. This control method was shown to be efficient at estimating the current atmospheric OPD state by the consideration of the current atmospheric conditions (i. e. the seeing) and compensating the time delay.⁶ Details about the requirements for the PSF fitting algorithm and the expected PSF images including detector noise and readout artefacts based on simulations are given in Horrobin et al.¹¹

In addition to the simulations a laboratory experiment including an interferometric beam combiner with controllable OPD is used to evaluate the control algorithms and to study realistic PSF images. Details of the experiment can be found in Bertram et al.¹⁸ and Rost et al.⁶ The first laboratory results indicate that it is not advisable to design the fringe loops solely on the basis of simulated PSF images.¹⁹

4. DISCUSSION

The control design of the FFTS is an ongoing process, as more and more data of vibrations and AO performance is gathered. The basic concept of splitting OPD control in atmospheric and instrumental parts allows a flexible handling of measurements. The integration of multiple sensors into a control scheme is a difficult task, e. g. the performance of the OVMS directly affects the performance of the fringe fitting, as with insufficient vibration control the fringe will be blurred, or the fringe contrast is decreased. Preliminary performance estimations can be found in Rost et al.,⁶ but a deeper understanding of the instrument, the behavior of the AO, detectors, actuators, and the telescope structure show a complex connection of the performance to the various subsystems. With the introduced control scheme it is possible to handle data from different sources with different reliability and optimize control parameters without the risk of losing flexibility under varying observing conditions.

ACKNOWLEDGMENTS

REFERENCES

- [1] Bertram, T., *Cophasing LINC-NIRVANA and Molecular gas in low-luminosity QSO host and cluster galaxies*, PhD thesis, Universität zu Köln (October 2007).
- [2] Bertram, T., Eckart, A., Lindhorst, B., Rost, S., Straubmeier, C., Wang, Y., Wank, I., Witzel, G., Beckmann, U., Brix, M., Egner, S., and Herbst, T. M., "The LINC-NIRVANA fringe and flexure tracking system," *Proc. SPIE* **7013-78** (2008).

- [3] Herbst, T. M., Ragazzoni, R., Eckart, A., and Weigelt, G., “The LINC-NIRVANA interferometric imager for the Large Binocular Telescope,” *Proc. SPIE* **5492**, 1045–1052 (Sept. 2004).
- [4] Herbst, T. M., Ragazzoni, R., Eckart, A., and Weigelt, G. P., “Imaging beyond the fringe: an update on the LINC-NIRVANA Fizeau interferometer for the LBT,” *Proc. SPIE* **7734-6** (2010).
- [5] Rost, S., Bertram, T., Straubmeier, C., Wang, Y., and Eckart, A., “The LINC-NIRVANA fringe and flexure tracker: piston control strategies,” *Proc. SPIE* **6274-1P** (2006).
- [6] Rost, S., Bertram, T., Lindhorst, B., Straubmeier, C., Wang, Y., Witzel, G., and Eckart, A., “The LINC-NIRVANA Fringe and Flexure Tracker: Testing Piston Control Performance,” *Proc. SPIE* **7013-118** (2008).
- [7] Bertram, T., Arcidiacono, C., Straubmeier, C., Rost, S., Wang, Y., and Eckart, A., “The LINC-NIRVANA fringe and flexure tracker: image analysis concept and fringe tracking performance estimate,” in [*Advances in Stellar Interferometry. Edited by Monnier, John D.; Schöller, Markus; Danchi, William C.. Proceedings of the SPIE, Volume 6268, pp. 62683P (2006).*], Presented at the Society of Photo-Optical Instrumentation Engineers (SPIE) Conference **6268** (July 2006).
- [8] Wang, Y., Bertram, T., Straubmeier, C., Rost, S., and Eckart, A., “The LINC-NIRVANA fringe and flexure tracker: Linux real-time solutions,” in [*Advanced Software and Control for Astronomy. Edited by Lewis, Hilton; Bridger, Alan. Proceedings of the SPIE, Volume 6274, pp. 62741O (2006).*], Presented at the Society of Photo-Optical Instrumentation Engineers (SPIE) Conference **6274** (July 2006).
- [9] Zuther, J., Eckart, A., Horrobin, M., Lindhorst, B., Lindhorst, U., Moser, L., Rost, S., Straubmeier, C., Tremou, E., Wank, I., and Bertram, T., “The LINC-NIRVANA fringe and flexure tracker: an update of the opto-mechanical system,” *Proc. SPIE* **7734-155** (2010).
- [10] Herbst, T. M., Ragazzoni, R., Eckart, A., and Weigelt, G. P., “LINC-NIRVANA: the Fizeau interferometer for the LBT,” *Proc. SPIE* **7013-77** (2008).
- [11] Horrobin, M., Eckart, A., Lindhorst, B., Lindhorst, U., Moser, L., Rost, S., Straubmeier, C., Tremou, E., Wank, I., and Zuther, J., “Fringe detection and piston variability in LINC-NIRVANA,” *Proc. SPIE* **7734-68** (2010).
- [12] Arcidiacono, C., Diolaiti, E., Ragazzoni, R., Farinato, J., and Vernet-Viard, E., “Sky coverage for layer-oriented mcao: a detailed analytical and numerical study,” *Advancements in Adaptive Optics* **5490**(1), 563–573, SPIE (2004).
- [13] Ciliegi, P., La Camera, A., Antonucci, S., Desidera, G., Bertero, M., Boccacci, P., Carbillet, M., Diolaiti, E., Foppiani, I., Lombini, M., Lorenzetti, D., Nisini, B., and Schreiber, L., “Analysis of LBT LINC-NIRVANA simulated images with the software package AIRY-LN,” *Proc. SPIE* **7734-88** (2010).
- [14] Brix, M., Pott, J., Bertram, T., Rost, S., Borelli, J. L., Esguerra, J. D., G”assler, W., Herbst, T. M., Kuerster, M., Naranjo, V., and Rohloff, R., “Linc-Nirvana piston control elements,” *Proc. SPIE* **7734-65** (2010).
- [15] Tremou, E., Eckart, A., Horrobin, M., Lindhorst, B., Moser, L., Rost, S., Straubmeier, C., Wank, I., and Zuther, J., “The LINC-NIRVANA fringe and flexure tracker: laboratory tests,” *Proc. SPIE* **7734-148** (2010).
- [16] Kuerster, M., Bertram, T., Borelli, J. L., Brix, M., G”assler, W., Herbst, T. M., Naranjo, V., Pott, J., Connors, T. E., Hinz, P. M., McMahon, T. J., Ashby, D. S., Brynnel, J. G., Edgin, T., Esguerra, J. D., Green, R. F., Kraus, J., Little, J., Cushing, N. J., Beckmann, U., and Weigelt, G. P., “OVMS: the optical path difference and vibration monitoring system for the LBT and its interferometers,” *Proc. SPIE* **7734-107** (2010).
- [17] Brix, M., Naranjo, V., Beckmann, U., Bertram, R., Bertram, T., Brynnel, J., Egner, S., Gaessler, W., Herbst, T. M., Kuerster, M., Rohloff, R. R., Rost, S., and Schmidt, J., “Vibration measurements at the Large Binocular Telescope (LBT),” *Proc. SPIE* **7012-92** (2008).
- [18] Bertram, T., Lindhorst, B., Tremou, E., Rost, S., Wang, Y., Witzel, G., Straubmeier, C., and Eckart, A., “The LINC-NIRVANA Fringe and Flexure Tracker: The testbed interferometer,” *Proc. SPIE* **7013-117** (2008).
- [19] Moser, L., Eckart, A., Horrobin, M., Lindhorst, B., Rost, S., Straubmeier, C., Tremou, E., Wank, I., Zuther, J., and Bertram, T., “The LINC-NIRVANA fringe and flexure tracker: first measurements of the testbed interferometer,” *Proc. SPIE* **7734-106** (2010).